

# Prefix-Free Code Distribution Matching for Probabilistic Constellation Shaping

Junho Cho, *Member, IEEE*

**Abstract**—In this work, we construct energy-efficient variable-to-fixed length (V2F), fixed-to-variable length (F2V), and variable-to-variable length (V2V) prefix-free codes, which are optimal (or near-optimal) in the sense that no (or few) other codes with the size can achieve a smaller energy per code letter for the same entropy rate. Under stringent constraints of 4096 entries or below per codebook, the constructed codes yield an energy per code letter within a few tenths of a dB of the *unconstrained* theoretic lower bound, across a wide range of entropy rates with a very fine granularity. We also propose a framing method that allows variable-length codes to be transmitted using a fixed-length frame. The penalty caused by framing is studied using simulations and analysis, showing that the energy per code letter is kept within 0.2 dB of the unconstrained theoretic limit for some tested codes with a large frame length. When framed prefix-free codes are used to implement probabilistic constellation shaping (PCS) for communications in the additive white Gaussian noise channel, simulations show that 1.1 dB and 0.65 dB of shaping gains are achieved relative to uniform 8- and 16-quadrature amplitude modulation (QAM), respectively.

**Index Terms**—Prefix-free codes, distribution matching, probabilistic constellation shaping.

## I. INTRODUCTION

PREFIX-free codes are generally used in *source coding* to transform source letters of an arbitrary probability distribution to code letters of a uniform probability distribution, thereby maximizing entropy per code letter. In this work, we use prefix-free codes for a reverse purpose, i.e., for an operation called *distribution matching (DM)* that transforms uniformly distributed source letters to code letters of a desired probability mass function (PMF). In particular, we restrict the source symbols to Bernoulli-distributed bits  $b \in \mathcal{B} := \{0, 1\}$  with equal probabilities  $\mathbb{P}(b = 0) = \mathbb{P}(b = 1) = 0.5$ , and construct prefix-free codes such that the code letters have the minimum average energy among all possible prefix-free codes of the same size for the desired entropy per code letter. We also propose a *framing* method, with which variable-length prefix-free codewords can always be contained in a fixed-length frame, thereby facilitating application of prefix-free codes to communications, as will be discussed below.

A prominent application of *prefix-free code distribution matching (PCDM)* is *probabilistic constellation shaping (PCS)* for capacity-approaching communications. PCS makes low-energy code letters appear with a higher probability than high-energy code letters, thereby reducing average transmit energy for the same *information rate (IR)* [1]–[11]. A long-standing challenge of PCS has been incorporation of channel coding and DM. If PCDM is embedded between channel encoding

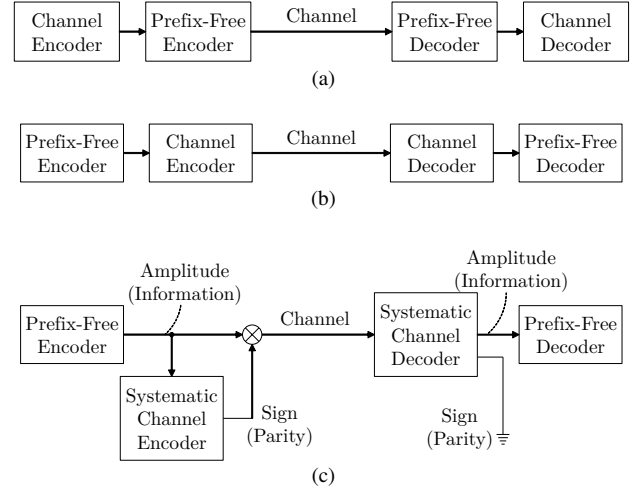


Fig. 1. Architectures for a coded modulation system.

and decoding (see Fig. 1 (a)), even a single error from the channel causes insertion or deletion of source letters in prefix-free decoding, leading to synchronization errors or catastrophic propagation of errors, thereby rendering the outer channel coding useless. In a reversed architecture where channel coding is embedded between prefix-free encoding and decoding (see Fig. 1 (b)), a symbol distribution formed by prefix-free encoding is not preserved by the subsequent channel encoding, since (linear) channel encoding generates almost equiprobable code symbols from source symbols of any distribution. There have been approaches to jointly optimizing channel coding and DM [6], [9]–[11], but they lack a rate adaptability and involve design of a customized channel coding scheme. Recently, however, an architecture called *probabilistic amplitude shaping (PAS)* [12] solved the problem. In the PAS architecture, source bits are first encoded by a prefix-free code to produce *amplitudes* of transmit symbols with a desired probability distribution, as shown in Fig. 1 (c), then a following systematic channel encoder generates parity bits that constitute *signs* of the transmit symbols. In this manner, the amplitude distribution remains unchanged by equiprobable parity bits, and the error propagation and synchronization errors do not occur since channel decoding corrects errors before prefix-free decoding. PAS enables separate design of channel coding and DM, hence allows for the use of off-the-shelf channel codes in conjunction with independently optimized prefix-free codes. In this paper, therefore, the performance of the proposed PCDM in communication systems will be numerically evaluated using the PAS architecture in comparison with the conventional communication schemes where transmit symbols

are uniformly distributed.

## II. PRIOR WORKS

Let  $\mathcal{X} := \{x_1, \dots, x_M\}$  be an  $M$ -ary code alphabet. Also, let  $\mathcal{B}^*$  and  $\mathcal{X}^*$ , respectively, denote a set of sourcewords (called a *dictionary*) that are concatenations of an indefinite number of source letters from alphabet  $\mathcal{B}$  and a set of codewords (called a *codebook*) that are concatenations of an indefinite number of code letters from alphabet  $\mathcal{X}$ . A code  $\mathcal{C} : \mathcal{B}^* \rightarrow \mathcal{X}^*$  defines a bijective function that maps every sourceword in  $\mathcal{B}^*$  to exactly one codeword in  $\mathcal{X}^*$  such that  $\mathcal{C}$  is *uniquely decodable*. If a codeword  $\mathbf{x} \in \mathcal{X}^*$  is an ordered concatenation of two non-empty words  $\mathbf{x}_{\text{pre}}$  and  $\mathbf{x}'$ , then  $\mathbf{x}_{\text{pre}}$  is called a *prefix* of the word  $\mathbf{x}$ . A code is a *prefix-free code* if any codeword  $\mathbf{x} \in \mathcal{X}^*$  is not a prefix of another codeword. A prefix-free code is an *instantaneously decodable code*, whose decoding can be performed as immediately as a codeword is found on successive receipt of the code letters. The *size* of a code is defined by the number of all codewords in the codebook, hence the number of all sourcewords in the dictionary.

In a special case where all code letters have equal transmit energies, *Huffman codes* represent optimal prefix-free codes for a known sourceword distribution, optimal in the sense that no other codes can produce a shorter expected codeword length. In a more general case where code letter energies are not necessarily equal, the prefix-free code construction problem has been addressed in the context of PCS in [13], using *Lempel-Even-Cohn (LEC)* coding [14] and *Varn coding* [2]. LEC coding solves the problem when all codewords have an equal length. LEC coding is isomorphic to Huffman coding if we translate the transmit energy  $w_n$  of the  $n$ -th codeword  $v_n$  into a sourceword probability as  $p_n = \alpha^{-w_n}$ , with  $\alpha$  being a root of  $\sum_{n=1}^N \alpha^{-w_n} = 1$  to ensure that PMF sums to 1. A Huffman codebook therefore becomes the LEC dictionary for parsing source bits, mapped to an LEC codebook consisting of equal-length codewords, completing a *variable-to-fixed length (V2F)* code. However, LEC coding minimizes the energy *per source letter*, and the entropy rate is determined by the *a priori* given Huffman codebook, while we want to minimize the energy *per code letter* for an arbitrary entropy rate. Varn coding provides another solution when sourcewords have an equal length, hence constructing *fixed-to-variable length (F2V)* codes. However, Varn coding requires a non-uniform PMF for the equal-length sourcewords, which must be given *a priori* to realize a particular entropy rate determined by the PMF. Another approach to constructing F2V codes is by minimizing the information divergence between the desired and realized PMFs for a binary code alphabet [15], which also assumes *a priori* knowledge of the optimal PMF for the desired entropy rate. In a general case where both sourcewords and codewords are allowed to have unequal lengths, there are known algorithms to construct optimal prefix-free codes [3], [16]–[19] using, e.g., dynamic programming [18], [19]; however, the resulting codes are optimal in terms of the energy *per codeword*, while we need a minimum energy *per code letter*. To the best of our knowledge, none of the existing

TABLE I  
EXAMPLES OF PREFIX-FREE CODES FOR 2-ASK CODE LETTERS.

<b>b</b>	<b>x</b>	<b>b</b>	<b>x</b>	<b>b</b>	<b>x</b>
0	111	000	1111111	0	1111111
100	113	001	1111113	100	1111113
101	131	010	111113	101	111113
110	311	011	11113	110	11113
1110	133	100	1113	1110	1113
11110	313	101	113	11110	113
111110	331	110	13	111110	13
111111	333	111	3	111111	3

(a) V2F

(b) F2V

(c) V2V

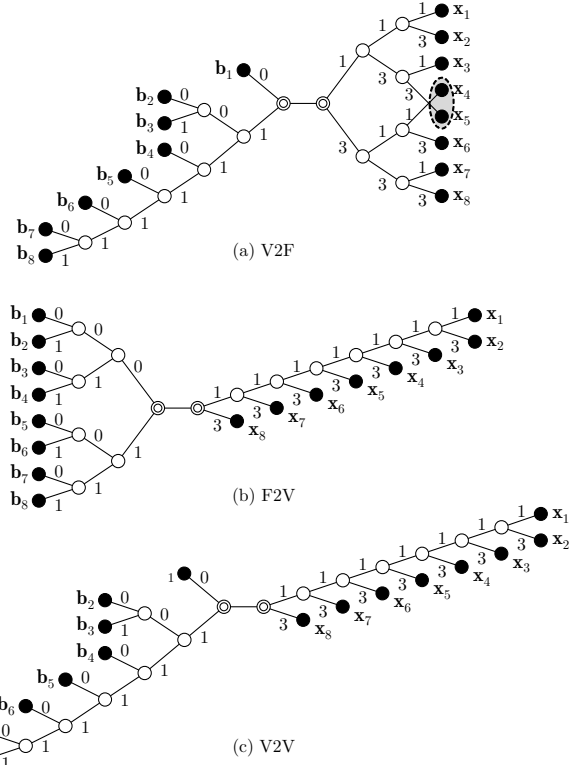


Fig. 2. Root-concatenated trees representing the codes in Tab. I.

approaches did not address the problem of constructing prefix-free codes that minimize the energy per code letter for arbitrary desired entropy rates.

## III. PREFIX-FREE CODES FOR VARIOUS ENTROPY RATES

Let  $u_n$  denote the length of sourceword  $\mathbf{b}_n$ , and  $v_n$  and  $w_n$  denote the length and energy of codeword  $\mathbf{x}_n$ , respectively. Let  $U$ ,  $V$ , and  $W$  be random variables taking values on the sets  $\{u_1, \dots, u_N\}$ ,  $\{v_1, \dots, v_N\}$ , and  $\{w_1, \dots, w_N\}$ , respectively, all of which are distributed with the PMF  $\mathbf{p} = [p_1, \dots, p_N]^T$ . Since our source bits are independent and equiprobable, the probability is *dyadic*, i.e.,  $p_n = 2^{-u_n}$  with  $\sum_{n=1}^N p_n = 1$ . Examples of size-8 V2F, F2V, and V2V codes for the unipolar 2-ary amplitude shift keying (2-ASK) code alphabet  $\mathcal{X}_{2\text{-ASK}} = \{1, 3\}$  are shown in Tab. I, where the V2V code has  $\mathbf{u} := [u_1, \dots, u_N]^T = [1, 3, 3, 3, 4, 5, 6, 6]^T$ ,  $\mathbf{v} := [v_1, \dots, v_N]^T = [7, 7, 6, 5, 4, 3, 2, 1]^T$ , and  $\mathbf{w} :=$

$[w_1, \dots, w_N]^T = [7, 15, 14, 13, 12, 11, 10, 9]^T$ . The corresponding tree diagrams are illustrated in Fig. 2, where double circles, open circles, and closed circles represent the root nodes, branch nodes, and leaf nodes, respectively, which will be defined below. A code is formed by concatenating the roots of two *ordered* trees, called *left* and *right trees* depending on their relative root position. We use the following terminologies throughout the paper to describe the structure of a right tree (defined in a similar fashion for a left tree):

- *Root*: The left-most node of a tree.
- *Child*: A node directly connected to the right of a node.
- *Parent*: The converse of a child.
- *Siblings*: A group of nodes with the same parent.
- *Branch*: A node with at least one child.
- *Leaf*: A node with no children.
- *Degree*: The number of children of a node.
- *Path*: A sequence of nodes and edges connecting a node with another node.
- *Depth*: The depth of a node is the number of edges from the root node to the node, i.e., the path length connecting the root node and the node.
- *Height*: The height of a tree is the longest path length between the root and leaves.
- *Size*: The size of a tree is the number of all leaf nodes of the tree.

Leaf  $n$  of a left tree represents sourceword  $\mathbf{b}_n$  and that of a right tree represents codeword  $\mathbf{x}_n$ . The depth of leaf  $n$  equals  $u_n$  (in the left tree) or  $v_n$  (in the right tree).

With the above notations, we can characterize energy and entropy rate of a root-concatenated tree. By the dyadic PMF of sourcewords and codewords, the expected energy per code letter can be calculated as

$$E := \frac{\mathbb{E}(W)}{\mathbb{E}(V)} = \frac{\sum_{n=1}^N 2^{-u_n} w_n}{\sum_{n=1}^N 2^{-u_n} v_n}, \quad (1)$$

where  $\mathbb{E}(\cdot)$  denotes expectation with respect to  $\mathbf{p}$  throughout the paper, unless otherwise specified. The entropy rate is defined as the expected number of source bits per code letter

$$R := \frac{\mathbb{E}(U)}{\mathbb{E}(V)} = \frac{\sum_{n=1}^N 2^{-u_n} u_n}{\sum_{n=1}^N 2^{-u_n} v_n}. \quad (2)$$

Then, the optimal prefix-free coding problem can be written as:

$$\begin{aligned} & \underset{\mathbf{u}, \mathbf{v}, \mathbf{w}}{\text{minimize}} && E \\ & \text{subject to} && R \geq R^*, \\ & && \mathbf{u}, \mathbf{v}, \mathbf{w} \text{ are the depth and energy vectors as defined.} \end{aligned} \quad (3)$$

#### A. V2F Codes

To solve the above problem, we begin with a *balanced*  $M$ -ary right tree, i.e., a right tree in which every branch has  $M$  children and every leaf is at the same depth (see the right tree of Fig. 2 (a)), which represents codebook  $\mathbf{X}$  of a fixed codeword length  $v_n = v$  for all  $n = 1, \dots, N$ , with  $N = M^v$ . Without loss of generality, assume that code letters are

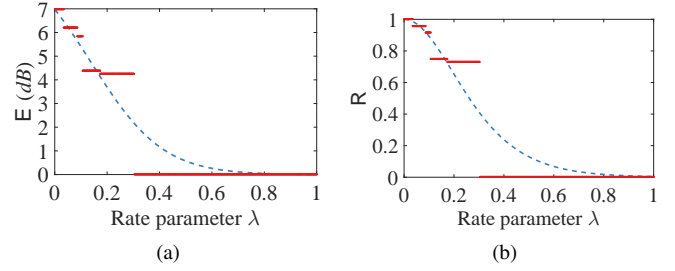


Fig. 3.  $E$  and  $R$  as a function of  $\lambda$ : (a)  $E$  of a continuous MB PMF (dashed lines) and its dyadic approximate (solid lines), relative to a uniform PMF, and (b) the corresponding  $R$ . The fixed-length codewords  $\mathbf{x}$  are given by Tab. I(a).

chosen from  $\mathcal{X}_{M\text{-ASK}} := \{1, 3, \dots, 2M - 1\}$  such that  $\mathbf{w}$  can immediately be obtained for the fixed  $v$ . In this case, (1) and (2) degenerate, respectively, to  $E_{V2F} = \frac{\mathbb{E}(W)}{v}$ , and  $R_{V2F} = \frac{\mathbb{E}(U)}{v} = \frac{\mathbb{H}(\mathbf{p})}{v}$ , where the last equation holds since  $\mathbf{p}$  is dyadic. Therefore, minimizing the expected energy *per code letter* is equivalent to minimizing the expected energy *per codeword* for V2F codes. Also, maximizing  $R_{V2F}$  subject to  $E_{V2F} \leq E^*$  is equivalent to maximizing  $\mathbb{H}(\mathbf{p})$  subject to  $\mathbb{E}(W) \leq vE^*$ .

If we waive the dyadic constraint on  $\mathbf{p}$ , the entropy-maximizing distribution under an energy constraint is the Maxwell-Boltzmann (MB) distribution [8], represented by a PMF  $\mathbf{p}_{\text{MB}} = [p_1^*, \dots, p_N^*]^T$  with  $p_n^* := \frac{\exp(-\lambda w_n)}{\sum_{i=1}^N \exp(-\lambda w_i)}$ ,  $n = 1, \dots, N$ , where the *rate parameter*  $\lambda \geq 0$  determines the expected energy per code letter. Let  $\mathbb{E}_{\mathbf{p}'}(\cdot)$  denote expectation with respect to a PMF  $\mathbf{p}'$ , then the energy per code letter and entropy rate of optimal V2F codes are given, respectively, by  $E_{\text{MB}} = \mathbb{E}_{\mathbf{p}_{\text{MB}}}(W)/v$  and  $R_{\text{MB}} = \mathbb{H}(\mathbf{p}_{\text{MB}})/v$ . Indeed, LEC coding [14] yields a special instance of the MB distribution, for which the rate parameter is given by  $\lambda = \log(\alpha)$  with  $\alpha$  being a root of the characteristic condition  $\sum_{n=1}^N \alpha^{-w_n} = 1$ . The dashed curves in Fig. 3 (a) and (b) show  $E_{\text{MB}}$  and  $R_{\text{MB}}$  as a strictly monotonically decreasing function of  $\lambda$  (this is true in general, see [12, Section 5.C]), obtained from the codewords of Tab. I (a). Due to the monotonicity, the optimal  $\lambda^*$  of the MB PMF that maximizes  $R_{\text{MB}}$  subject to  $E_{\text{MB}} \leq E^*$  can simply be obtained by the *bisection* method. Then, an optimal dyadic approximate  $\mathbf{p}$  of  $\mathbf{p}_{\text{MB}}$  can be obtained by *Geometric Huffman coding (GHC)* [20], i.e.,  $\mathbf{p} = \text{GHC}(\mathbf{p}_{\text{MB}})$ . Notice that, since code alphabet  $\mathcal{X}$  and constant  $v$  completely define the right tree of a V2F code, the optimal  $\mathbf{p}_{\text{MB}}$  can immediately be obtained for an arbitrary desired entropy rate  $R^*$ , using a series of operations  $(\mathcal{X}, v, R^*) \mapsto \mathbf{p}_{\text{MB}} \mapsto \mathbf{p} \mapsto (E_{V2F}, R_{V2F})$ . The solid lines in Figs. 3 (a) and (b) show all  $E_{V2F}$  and  $R_{V2F}$  obtained with  $\mathcal{X}_{2\text{-ASK}}$  and  $v = 3$ . In this example, there are only five non-zero distinct rates generated by dyadic approximation of  $\mathbf{p}_{\text{MB}}$ . As we increase the codebook size, the entropy rates created by V2F codes become much more diverse, as shown in Fig. 4 for up to the 16-ASK alphabet (producing up to the 1024-QAM in the PAS architecture). Here, we find all V2F codes from the desired entropy rates  $R^* \in \{\Delta, 2\Delta, \dots, \log_2 M\}$  with a rate granularity  $\Delta = 0.001$ . The entropy rates become sparser in relatively low entropy rate regimes, which can be supplemented by allowing variable codeword lengths in Section III-C.] Energy efficiency of the

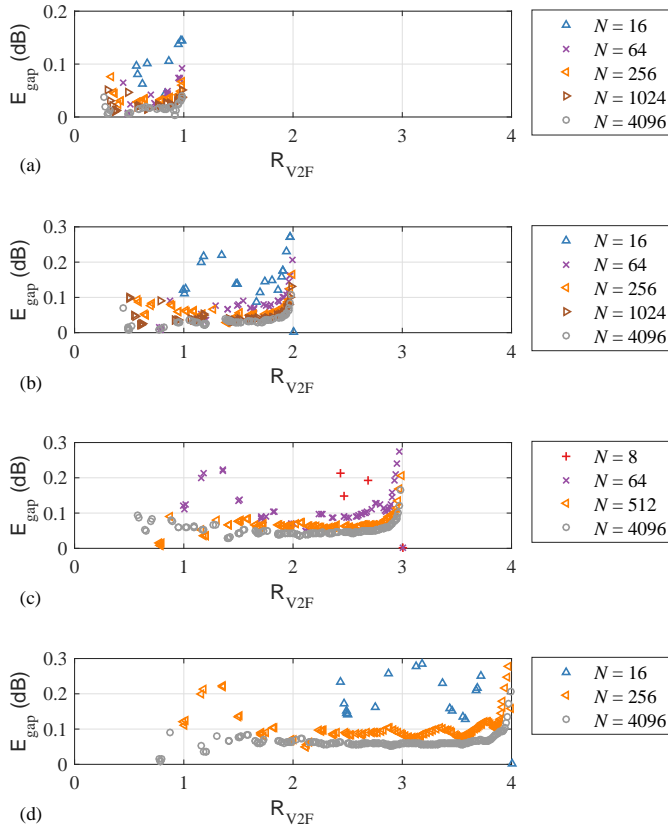


Fig. 4. Energy gap of V2F codes for  $N \leq 4096$  with the (a) 2-ASK, (b) 4-ASK, (c) 8-ASK, and (d) 16-ASK alphabets.

constructed V2F codes are also shown in Fig. 4, evaluated by the ratio of the energy per code letter of the prefix-free code to that of the ideal MB-distributed code letters for the same entropy rate, i.e.,  $E_{\text{gap}} := \frac{E_{\text{V2F}}}{E_{\text{MB}}}$ , which we call *energy gap*. It can be seen that the energy gap is below 0.1 dB across a wide range of entropy rates with  $N \leq 4096$ , or even with  $N \leq 64$  for  $M \leq 4$ .

### B. F2V Codes

For F2V codes, now we consider a balanced binary left tree representing dictionary  $\mathbf{B}$  of fixed sourceword length  $u_n = u$  for all  $n = 1, \dots, N$ , with  $N = 2^u$ , such that all  $\mathbf{b}_n \in \mathbf{B}$  are parsed with equal probabilities  $p_n = 2^{-u}$ . In this case, the expected energy per code letter and entropy rate of a code are simplified, respectively, as

$$E_{\text{F2V}} = \frac{\mathbb{E}(W)}{\mathbb{E}(V)} = \frac{\omega}{\nu}, \quad (4)$$

and

$$R_{\text{F2V}} = \frac{u}{\mathbb{E}(V)} = \frac{2^u u}{\nu}, \quad (5)$$

with *sum depth* and *sum energy* of the tree being  $\nu := \sum_{n=1}^N v_n$  and  $\omega := \sum_{n=1}^N w_n$ , respectively.

We do not know of any existing method that can solve (3) with (4) and (5) for an arbitrary desired  $R^*$ . In this paper, therefore, instead of directly solving the problem for a particular  $R^*$ , we try to identify a set of trees that produces all possible

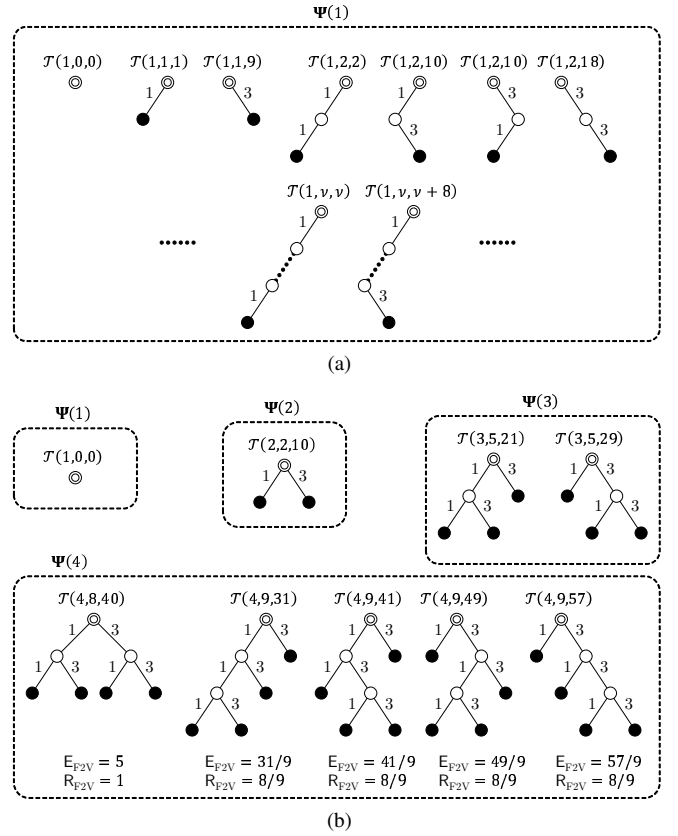


Fig. 5. All  $L^+$ -trees in  $\Psi(N)$  with the 2-ASK alphabet for (a)  $L = 1, N = 1$ , and (b)  $L = 2, N \leq 4$ .

sum depths  $\nu$  under a finite tree size constraint, hence realizing all possible  $R_{\text{F2V}}$  according to (5). The constructed trees are optimal in the sense that they have the minimum sum energy  $\omega$  among all  $2^+$ -trees with the same sum depth  $\nu$ , where  $L^+$ -tree is a tree in which every node except leaves has a degree not smaller than  $L$ . Minimum sum energy of a tree leads to minimum energy per code letter for a given  $\nu$ , and for a given  $R_{\text{F2V}}$  due to (4) and (5). Indeed, any  $1^+$ -tree is allowed for a right tree; however, we restrict the type of trees to  $2^+$ -trees to avoid infinite tree expansion (see Fig. 5 (a) for example). In Fig. 5, and throughout the paper,  $\mathcal{T}(N)$  denotes a tree that has  $N$  leaves,  $\mathcal{T}(N, \nu)$  is a tree  $\mathcal{T}(N)$  whose sum depth is  $\nu$ , and  $\mathcal{T}(N, \nu, \omega)$  is a tree  $\mathcal{T}(N, \nu)$  whose sum energy is  $\omega$ . Also, let  $\Psi(N)$  and  $\Psi(N, \nu)$  be the sets of all trees  $\mathcal{T}(N)$  and  $\mathcal{T}(N, \nu)$ , respectively. Then, by (4) and (5), all trees in  $\Psi(N, \nu)$  lead to same  $R_{\text{F2V}}$  but not necessarily same  $E_{\text{F2V}}$ . Since distinct sum depth  $\nu$  generates distinct  $R_{\text{F2V}} = \frac{2^u u}{\nu}$ , we have as many optimal trees as the number of distinct sum depths of trees in  $\Psi(N)$ , where an optimal tree with sum depth  $\nu$  is defined as  $\mathcal{T}^*(N, \nu) = \arg\min_{\mathcal{T}(N, \nu) \in \Psi(N, \nu)} \omega$ . A brute-force search of  $\mathcal{T}^*(N, \nu)$  in  $\Psi(N)$  requires exponential time in  $N$ . There are known problems that are isomorphic to the problem of counting the number of all trees in  $\Psi(N)$ , including the parenthesizations counting problem [21, Ch. 15.2]. For example, the trees in  $\Psi(4)$  of Fig. 5 (b) have isomorphic representations of  $((13)(13))$ ,  $((13)3)3$ ,  $((1(13))3)$ ,  $(1((13)3))$ , and  $(1(1(13)))$  in order, in which the edges connecting two siblings are parenthesized together in

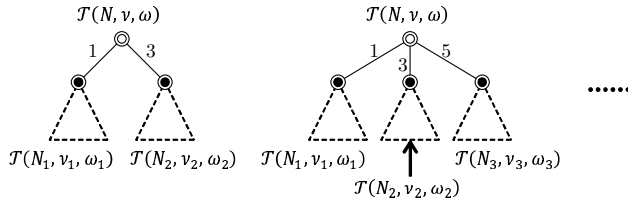


Fig. 6. A large tree constructed from smaller sub-trees.

a recursive manner from the largest depth of the tree. The number of parenthesizations for  $\Psi(N)$  is  $C_{N-1}$ , with  $C_N$  being the *Catalan number* defined as  $C_N := \frac{(2N)!}{N!(N+1)!}$  [22], [23], which grows as  $\Omega(\frac{4^N}{N^{3/2}})$  [21, p. 333].

In order to reduce the search space, we take a *dynamic programming* approach, as suggested in [18], [19] to find a prefix-free code for a known codeword PMF. We begin from a trivial size-1 tree that has only a root, then construct larger trees by appending smaller trees to the root, as shown in Fig. 6. A tree  $\mathcal{T}(N, \nu, \omega)$  formed by appending sub-trees  $\mathcal{T}(N_k, \nu_k, \omega_k)$ ,  $k = 1, \dots, K$  satisfies the following relations:

$$N = \sum_{k=1}^K N_k, \quad (6)$$

$$\nu = \sum_{k=1}^K N_k + \sum_{k=1}^K \nu_k = N + \sum_{k=1}^K \nu_k, \quad (7)$$

$$\omega = \sum_{k=1}^K (2k-1)^2 N_k + \sum_{k=1}^K \omega_k, \quad (8)$$

where the last two equations hold since the  $k$ -th edge from the root should be taken into account  $N_k$  times to calculate sum depth and sum energy of the tree. For example, due to (6), a tree with  $N = 4$  and the 4-ASK alphabet (hence  $2 \leq K \leq 4$ ) can be constructed from  $K$ -tuples:  $(N_1, N_2) = (1, 3), (2, 2), (3, 1)$  for  $K = 2$ ,  $(N_1, N_2, N_3) = (1, 1, 2), (1, 2, 1), (2, 1, 1)$  for  $K = 3$ , and  $(N_1, N_2, N_3, N_4) = (1, 1, 1, 1)$  for  $K = 4$ . Here, we do not need to use all sub-trees of size  $< N$  to construct a set of size- $N$  trees, since we have an *optimal sub-substructure* property:

**Theorem 1.** An optimal tree  $\mathcal{T}^*(N)$  contains only optimal sub-trees  $\mathcal{T}^*(n < N)$  in it.

*Proof:* Suppose that an optimal tree  $\mathcal{T}^*(N, \nu, \omega^*)$  has a  $k$ -th sub-tree  $\mathcal{T}(N_k, \nu_k, \omega_k)$ . If the sub-tree  $\mathcal{T}(N_k, \nu_k, \omega_k)$  is not an optimal tree, then there exists a sub-tree  $\mathcal{T}^*(N_k, \nu_k, \omega_k^*)$  with  $\omega_k^* < \omega_k$ . By replacing the sub-tree  $\mathcal{T}(N_k, \nu_k, \omega_k)$  with  $\mathcal{T}^*(N_k, \nu_k, \omega_k^*)$  from the tree  $\mathcal{T}^*(N, \nu, \omega^*)$ , we can obtain a new tree  $\mathcal{T}'(N, \nu, \omega')$  that has a smaller sum energy than the optimal tree, i.e., with  $\omega' < \omega^*$ . This is contradiction, hence an optimal tree consists of only optimal sub-trees. ■

It can be easily seen that the height of  $\mathcal{T}(N)$  is minimized when its leaves have maximally uniform depths. The depths can differ from each other at most by one, and the minimum height is given by  $\lceil \log_M N \rceil$  for the  $M$ -ASK alphabet. The sum depth of a size- $N$  minimum-height tree is calculated as  $\nu_{\min} := (N - M^{\lceil \log_M N \rceil})(\lceil \log_M N \rceil + 1) + M^{\lceil \log_M N \rceil} \lceil \log_M N \rceil$ , which is equal to the smallest sum depth

of all trees in  $\Psi(N)$ . If  $N$  is a positive integer power of  $M$ , the minimum sum depth can be simplified as  $\nu_{\min} = N \log_M N$ . On the other hand, if there are only two nodes at every depth of a tree (see, e.g., the last tree of Fig. 5 (b)), the tree has height  $N - 1$  that is the largest of all trees in  $\Psi(N)$ . The sum depth in this case is calculated as  $\nu_{\max} = \sum_{v=1}^{N-1} v + (N-1) = \frac{(N+2)(N-1)}{2}$ . After some manipulation, it can be seen that the sum depth of a maximum-height tree is also the maximum sum depth of all trees in  $\Psi(N)$ . Therefore, if we store only one optimal tree to  $\Psi^*(N)$  for each  $\nu$ , the size of  $\Psi^*(N)$  is upper-bounded by  $\nu_{\max} - \nu_{\min} + 1 = \frac{N^2}{2} + O(N \log_M N)$ ; i.e.,  $|\Psi^*(N)|$  grows as  $O(N^2)$ . Since there are at most  $N$  choices of the optimal sub-tree sets (ranging from an empty set to  $\Psi^*(N-1)$ ) for each of the  $M$  edges of the root for enumerating all trees of size  $N$  (using the optimal sub-tree property), the number of all choices to build  $\Psi(N)$  is of the complexity  $\Omega(N^M)$ . As aforementioned, each of the sub-tree sets is of size at most  $\Omega(N^2)$ , hence we have the search space of size  $\Omega(N^{M+2})$  to identify  $\Psi^*(N)$ . The search time is polynomial in  $N$ , and exponential in  $M$ , indicating the intractability of constructing F2V codes for a large alphabet.

To further reduce the search space, we can exploit the fact that a larger sub-tree is appended as far left as possible from the root of an optimal tree; i.e.,

**Theorem 2.** Let  $\mathcal{T}_k$  for  $k = 1, \dots, K$  constitute the  $k$ -th sub-tree of an optimal tree  $\mathcal{T}^*$  such that the root of  $\mathcal{T}_k$  is the  $k$ -th child of the root of  $\mathcal{T}^*$ , then the sub-trees satisfy  $|\mathcal{T}| > |\mathcal{T}_1| \geq \dots \geq |\mathcal{T}_K|$ .

*Proof:* Let  $\mathcal{T}(N_i, \nu_i)$  and  $\mathcal{T}(N_j, \nu_j)$  denote two of the sub-trees of an optimal tree  $\mathcal{T}^*(N, \nu)$  with  $i < j$ , and assume  $N_i < N_j$ . Then, by exchanging the two sub-trees  $\mathcal{T}(N_i, \nu_i)$  and  $\mathcal{T}(N_j, \nu_j)$ , we can construct another tree  $\mathcal{T}'(N, \nu)$  of the same size  $N$  and the same sum depth  $\nu$  due to (6) and (7), which has a smaller sum energy than  $\mathcal{T}^*(N, \nu)$  by (8). This is contradiction, hence an optimal tree must have  $N_i \geq N_j$  for any  $i > j$ . ■

For example, some trees in  $\Psi(4)$  can be generated from three sub-trees that have  $(N_1, N_2, N_3) = (2, 1, 1), (1, 2, 1)$ , or  $(1, 1, 2)$ , but we can discard the latter two triplets by Theorem 2.

We construct one optimal F2V code for each of the entropy rates that can be realized with  $N \leq 64$  for  $\mathcal{X}_{2\text{-ASK}}$  and  $\mathcal{X}_{4\text{-ASK}}$ . As shown in Fig. 7, F2V codes offer a greater diversity of entropy rates than V2F codes with the same size, albeit with a slightly larger energy gap. Therefore, a natural consequence is to construct V2V codes to exploit the complementary merits of V2F and F2V codes, as will be illustrated henceforth.

### C. V2V Codes

We readily have a set  $\Psi_R^*(N)$  of optimal right trees, representing optimal F2V codes. From this, without imposing any fixed-length constraints on source words and codewords, we can enumerate near-optima V2V codes of size  $N$  in the following manner:

- 1) For each of the desired entropy rates  $R^* = k\Delta_R$ , where  $k = 1, \dots, K$  for some integer  $K$  and the *rate*

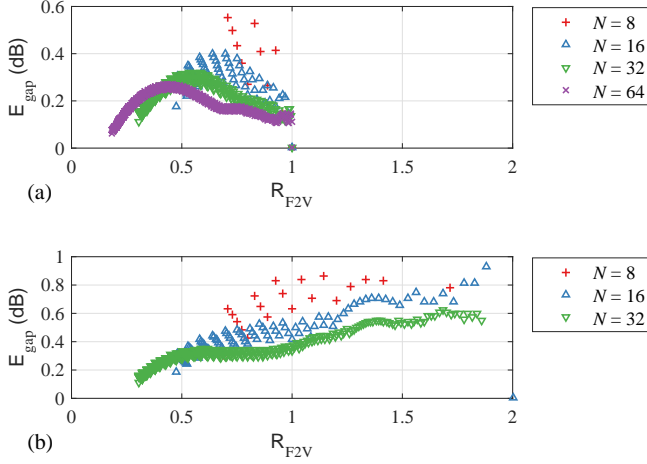


Fig. 7. Energy gap of all F2V codes (a) for  $N \leq 64$  with the 2-ASK alphabet, and (b) for  $N \leq 32$  with the 4-ASK alphabet.

granularity  $\Delta_R = \frac{\log_2 M}{K}$ , and for each of the optimal right trees in  $\Psi_R^*$ , identify the optimal PMF  $\mathbf{p}^*$  that achieves  $R^*$  with the minimum energy per code letter.

- 2) For every  $\mathbf{p}^*$  obtained in Step 1, construct a set of optimal left trees  $\Psi_L^*$  representing  $\mathbf{p} = \text{GHC}(\mathbf{p}^*)$  that minimizes  $\mathbb{D}(\mathbf{p} \parallel \mathbf{p}^*)$ . The trees in  $\Psi_L^*$  and  $\Psi_R^*$  have one-to-one correspondence.
- 3) For each of  $R^* = k\Delta_R$ , choose a pair of left and right trees in  $\Psi_L^*$  and  $\Psi_R^*$  that yield the minimum energy per code letter with a rate discrepancy  $|R_{V2V} - R^*| < \delta$  for a small  $\delta$ .

Indeed, an optimal V2V code does not necessarily consist of an optimal right tree, hence an exhaustive search of the left tree should be performed over *all* right trees in  $\Psi_R(N)$ . However, due to the exponential growth of  $|\Psi_R|$  in  $N$ , we restrict the search space to optimal right trees in  $\Psi_R^*$ ; under this constraint, the constructed V2V codes show surprisingly good performance with a very small  $N \leq 32$ .

Assume that a right tree  $\mathcal{T}^*(N)$  is chosen from  $\Psi_R^*(N)$  (hence  $\mathbf{v}$  and  $\mathbf{w}$  are given). Then, from (2), we have  $R = \frac{-\sum_{n=1}^N p_n \log_2 p_n}{\sum_{n=1}^N p_n v_n} \geq R^* \Leftrightarrow -\sum_{n=1}^N p_n \log_2 \frac{p_n}{2^{-R^* v_n}} \geq 0$ . Let  $q_n := 2^{-R^* v_n}$ ,  $\mathbf{q} = [q_1, \dots, q_N]^T$ , then we have an equivalence relation by definition  $\mathbb{D}(\mathbf{p} \parallel \mathbf{q}) := \sum_{n=1}^N p_n \log_2 \frac{p_n}{q_n}$  as

$$R \geq R^* \Leftrightarrow -\mathbb{D}(\mathbf{p} \parallel \mathbf{q}) \geq 0. \quad (9)$$

Therefore, by waiving the dyadic constraint on  $\mathbf{p}$ , the optimization problem of (3) translates into

$$\begin{aligned} \underset{\mathbf{p}}{\text{minimize}} \quad & E = \frac{\sum_{n=1}^N p_n w_n}{\sum_{n=1}^N p_n v_n} \end{aligned} \quad (10)$$

$$\text{subject to} \quad -\mathbb{D}(\mathbf{p} \parallel \mathbf{q}) \geq 0, \quad (11)$$

$$\sum_{n=1}^N p_n = 1. \quad (12)$$

Let  $E^*$  denote the minimum energy found by solving (10)-(12), then, the optimal PMF is given by the solution of a convex

---

#### Algorithm 1 Finding an optimal codeword PMF $\mathbf{p}^*$ for $R^*$

---

**Input:**  $N, \mathbf{v}, \mathbf{w}, \mathbf{q}$

**Output:**  $\mathbf{p}^*$

*Initialization:*

$$\ell \leftarrow 0, \mathbf{p}^{(\ell)} \leftarrow \mathbf{q} / \sum_{n=1}^N q_n, E^{(\ell)} \leftarrow \mathbb{E}_{\mathbf{p}^{(\ell)}}(W) / \mathbb{E}_{\mathbf{p}^{(\ell)}}(V).$$

1: **repeat**

2:  $\ell \leftarrow \ell + 1$

3:  $\mathbf{p}^{(\ell)} \leftarrow \underset{\mathbf{p}}{\text{argmin}} [\mathbb{E}(W) - E^{(\ell-1)} \cdot \mathbb{E}(V)]$

subject to  $-\mathbb{D}(\mathbf{p} \parallel \mathbf{q}) \geq 0, \sum_{n=1}^N p_n = 1.$

4:  $E^{(\ell)} \leftarrow \mathbb{E}_{\mathbf{p}^{(\ell)}}(W) / \mathbb{E}_{\mathbf{p}^{(\ell)}}(V).$

5: **until**  $E^{(\ell-1)} - E^{(\ell)} < \varepsilon$

6: **return**  $\mathbf{p}^* \leftarrow \mathbf{p}^{(\ell)}$

---

optimization problem

$$\mathbf{p}^* = \underset{\mathbf{p}}{\text{argmin}} [\mathbb{E}(W) - E^* \cdot \mathbb{E}(V)], \quad (13)$$

since

$$E = \frac{\mathbb{E}(W)}{\mathbb{E}(V)} \geq E^* \Leftrightarrow \mathbb{E}(W) - E^* \mathbb{E}(V) \geq 0, \quad (14)$$

where the equality in the right-hand side equation holds if and only if  $E = E^*$ . Also, the constraint functions in (11) and (12) are concave and affine, respectively, hence the problem can efficiently be solved by a convex optimization solver such as the CVX [24], [25], on condition that  $E^*$  is known. Since we do not know of  $E^*$ , we can make an initial guess  $E^{(0)} = \mathbb{E}(W) / \mathbb{E}(V)$  using a PMF  $\mathbf{p} = \frac{\mathbf{q}}{\sum_{n=1}^N q_n}$ , then attempt to reduce the error between the energy estimate  $E^{(\ell)}$  of iteration  $\ell$  and the true minimum energy  $E^*$  in an iterative manner. This initial PMF maximizes  $-\mathbb{D}(\mathbf{p} \parallel \mathbf{q})$  in order to satisfy the rate condition (9), where the maximization of  $-\mathbb{D}(\mathbf{p} \parallel \mathbf{q})$  by the initial guess  $\mathbf{p}$  can be proven by using a Lagrangian  $\mathbb{L}(\mathbf{p}, \lambda) = -\mathbb{D}(\mathbf{p} \parallel \mathbf{q}) + \lambda(\sum_{n=1}^N p_n - 1)$ . By the Karush-Kuhn-Tucker (KKT) conditions [26, Ch. 5.5.3], a PMF  $\mathbf{p}$  maximizes  $-\mathbb{D}(\mathbf{p} \parallel \mathbf{q})$  if the gradient of the Lagrangian vanishes at  $\mathbf{p}$ ; i.e.,

$$\frac{\partial \mathbb{L}(\mathbf{p}, \lambda)}{\partial p_n} = -\log_2 \frac{p_n}{q_n} - \log_2 e + \lambda = 0$$

$$\Leftrightarrow \log_2 \frac{p_n}{q_n} = \lambda - \log_2 e$$

$$\Leftrightarrow p_n = 2^{\lambda - \log_2 e} q_n = r q_n \text{ for some constant } r.$$

Since  $\mathbf{p}$  is a PMF, we have that  $r = 1 / \sum_{n=1}^N q_n$  in the last equation, hence the PMF that maximizes  $-\mathbb{D}(\mathbf{p} \parallel \mathbf{q})$  is given by the initial guess  $\mathbf{p}$ . If this  $\mathbf{p}$  does not fulfill the rate condition (9), then no other PMF can satisfy it, hence the corresponding right tree should be discarded. Otherwise, we can solve the convex optimization problem iteratively until the estimation error  $E^{(\ell)} - E^*$  at iteration  $\ell$  reaches within a termination threshold  $\varepsilon > 0$ , as shown in Algorithm 1.

**Theorem 3.** Given a right tree  $\mathcal{T}(N)$ , Algorithm 1 produces PMF  $\mathbf{p}^*$  that is asymptotically optimal in iteration  $\ell$  for an entropy rate  $R \geq R^*$ , such that  $E$  approaches to  $E^*$ .



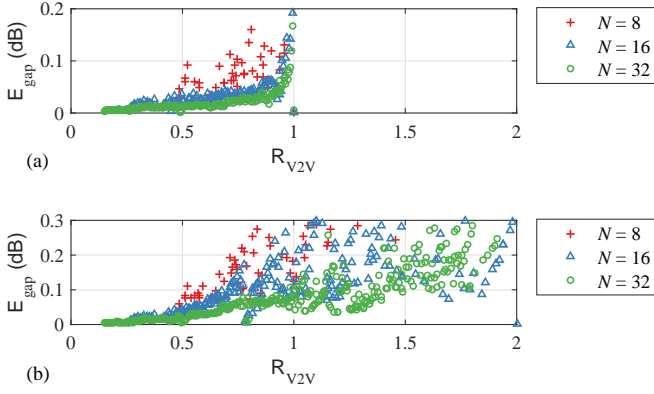


Fig. 8. Energy gap of V2V codes for  $N \leq 32$  with the (a) 2-ASK, and (b) 4-ASK alphabets.

*Proof:* The proof follows a similar structure to that of Proposition 4.5 in [27, Sec. 4.3.1]. Suppose that Algorithm 1 terminates at the iteration  $L$ . Then,  $E^{(\ell)}$  converges to  $E^{(L)}$  as  $\ell$  increases, since the termination condition on Line 5 is not satisfied at every  $\ell < L$ , hence  $E^{(\ell)} \leq E^{(\ell-1)} - \varepsilon$  for  $\ell < L$ , indicating that  $E^{(\ell)}$  is a monotonically decreasing function of  $\ell$ , while  $E^{(\ell)}$  is lower-bounded by  $E^*$ . Furthermore, the converged energy  $E^{(L)}$  is indeed the minimum energy  $E^*$  within a small error. To see this, let  $\Delta^{(\ell)} := \min_{\mathbf{p}} [\mathbb{E}(W) - E^{(\ell-1)} \cdot \mathbb{E}(V)]$  be the optimal value of the objective function at the iteration  $\ell$  such that  $\mathbb{E}(W) - E^{(\ell-1)} \cdot \mathbb{E}(V) \geq \Delta^{(\ell)}$  for any PMF  $\mathbf{p}$ , where the equality holds if and only if  $\mathbf{p} = \mathbf{p}^{(\ell)}$ . Then,  $\Delta^{(\ell)} \leq 0$ , since  $E^{(\ell-1)} \geq E^*$  for any PMF  $\mathbf{p}$ , where the equality holds if and only if  $E^{(\ell-1)} = E^*$  by (14). Also, since  $\mathbb{E}_{\mathbf{p}^{(\ell)}}(W) - E^{(\ell-1)} \cdot \mathbb{E}_{\mathbf{p}^{(\ell)}}(V) = \Delta^{(\ell)} \Leftrightarrow E^{(\ell-1)} - E^{(\ell)} = -\frac{\Delta^{(\ell)}}{\mathbb{E}_{\mathbf{p}^{(\ell)}}(V)}$ , the termination of Algorithm 1 at the iteration  $L$  implies  $-\frac{\Delta^{(L)}}{\mathbb{E}_{\mathbf{p}^{(L)}}(V)} < \varepsilon \Leftrightarrow \Delta^{(L)} > -\varepsilon \cdot \mathbb{E}_{\mathbf{p}^{(L)}}(V) \geq -\varepsilon \cdot \min_n v_n$ . This proves that Algorithm 1 can approach to the minimum energy  $E^*$  closely by choosing a sufficiently small  $\varepsilon$ , since  $\Delta^{(L)} \leq 0$  and  $\Delta^{(L)} = 0$  is a necessary and sufficient condition for  $E^{(L-1)} = E^*$ . ■

In our V2V code construction, Algorithm 1 is terminated mostly in 5 iterations with  $\varepsilon = 10^{-10}$ .

Once the optimal PMF  $\mathbf{p}^*$  is identified for every optimal right tree and for every desired entropy rates  $R^* = k\Delta_R$ , an optimal dyadic estimate can be obtained as  $\mathbf{p} = \text{GHC}(\mathbf{p}^*)$ , which creates a left tree. Then, among all pairs of such constructed left and right trees, a pair can be chosen for each entropy rate that achieves the minimum  $E$ .

Figure 8 shows all V2V codes enumerated by the rate granularity  $\Delta_R = 0.005$  and the rate tolerance  $\delta = 0.0025$  for the 2-ASK and 4-ASK alphabets with  $N = 8, 16, 32$ . For the 2-ASK alphabet, only  $N = 16$  is required to construct V2V codes to approach the theoretic minimum energy to within 0.05 dB across a wide range of entropy rates. For the 4-ASK alphabet, V2V codes are still within 0.1 to 0.2 dB of the limit across a wide range of entropy rates, although the obtained entropy rates are sparser and  $E_{\text{gap}}$  tends to grow with  $R_{V2V}$ . Some codes selected from Figs. 4 and 8 are shown in Fig. 9, whose entropy rates range from 0.15 to 3.83 in a step size

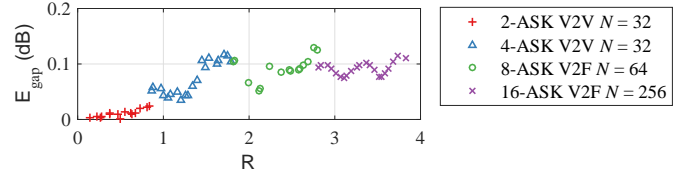


Fig. 9. Selected prefix-free codes for the 2-, 4-, 8-, and 16-ASK alphabets.

of  $\leq 0.016$ . This shows that we can approach the theoretic minimum energy per code letter to within 0.13 dB across a wide range of entropy rates for up to 1024-QAM, using a codebook size not larger than 256.

#### IV. FRAMING FOR FIXED-RATE TRANSMISSION

A fundamental problem of PCDM is that the number of output code letters varies depending on input patterns; i.e., the entropy rate of a prefix-free code is inherently *probabilistic*, whose mean value approaches to  $R$  asymptotically in the number of encoding iterations. Application of PCDM to data transmission is critically hampered by this, since it can cause buffer over- or under-flow, insertion or deletion of bits that causes synchronization errors, and unbounded error propagation in the absence of re-synchronization [8]. *Framing* in this paper refers to a method that enables a fixed-length frame to always contain a fixed number of information bits, thereby solving the variable length problem of PCDM. In [28, Sec. 4.8], framing is performed by casting overflow symbols into errors; the probability of error decreases as the frame length grows, but zero-error prefix-free decoding is not possible within a finite-length frame. To the best of our knowledge, there is no framing method known to date that allows unique error-free decoding of prefix-free codes.

##### A. Algorithm for Framing

To achieve a fixed entropy rate  $R_{\text{Frame}} < \log_2 M$  in each fixed-length frame for the  $M$ -ASK alphabet, we use two different codes: a prefix-free code  $\mathcal{C}_1$  with a probabilistic entropy rate whose mean value  $R_1$  is close to  $R_{\text{Frame}}$ , and a trivial code  $\mathcal{C}_2$  with a constant entropy rate  $R_2 = \log_2 M > R_1$  (i.e.,  $\mathcal{C}_2$  is a typical fixed-to-fixed length mapper for uniform  $M$ -ASK). The idea is that we begin encoding with  $\mathcal{C}_1$  and then *switch* to  $\mathcal{C}_2$  at some point of the successive encoding process if an overflow is predicted. If we keep counting the numbers of input bits and output symbols encoded by  $\mathcal{C}_1$  in the first part of the encoding process, we can also calculate the number of symbols required to encode all the remaining input bits if we use  $\mathcal{C}_2$  instead of  $\mathcal{C}_1$  from that point onward, thereby predicting a potential overflow. In what follows, we will show that this prediction can be made in a way that unique decoding is possible, and that the penalty due to this switching is small.

Let  $S$  (bits) and  $T$  (symbols) be fixed input and output frame lengths, respectively. Then, framing enables PCDM to achieve a fixed entropy rate  $R_{\text{Frame}}$ , where

$$R_1 < R_{\text{Frame}} := \frac{S}{T} \text{ (bits/symbol)} < R_2 \quad (15)$$

in each frame. This shows that, for the chosen  $R_1$  and  $R_2$ , an additional rate adaptability is also offered by framing, albeit with a small loss of energy efficiency. Let  $u^{(\ell)}$  and  $v^{(\ell)}$  denote the lengths of sourcewords and codewords of  $\mathcal{C}_1$  at encoding iteration  $\ell$ , respectively, then the *cumulative* sourceword and codeword lengths at iteration  $\ell$  can be calculated respectively as  $s^{(\ell)} := \sum_{i=1}^{\ell} u^{(i)}$ , and  $t^{(\ell)} := \sum_{i=1}^{\ell} v^{(i)}$ .

Assume that the use of  $\mathcal{C}_1$  up to iteration  $\ell - 1$  was assured not to cause overflow as long as we switch to  $\mathcal{C}_2$  from the next iteration  $\ell$  onwards, hence we have used  $\mathcal{C}_1$  up to iteration  $\ell - 1$ . Then, at the next iteration  $\ell$ , in order to foresee if  $\mathcal{C}_1$  does not still cause overflow, we need to ensure that

$$\gamma_{\text{Ava}}^{(\ell)} \geq \gamma_{\text{Req}}^{(\ell)}, \quad (16)$$

where  $\gamma_{\text{Ava}}^{(\ell)} := T - t^{(\ell)}$  and  $\gamma_{\text{Req}}^{(\ell)} := \left\lceil \frac{S - s^{(\ell)}}{R_2} \right\rceil$  define the available and required numbers of symbols in case we switch to  $\mathcal{C}_2$  after encoding with  $\mathcal{C}_1$  at  $\ell$ , respectively. Codebook  $\mathcal{C}_1$  is used for encoding at iteration  $\ell$  if condition (16) is fulfilled, otherwise  $\mathcal{C}_2$  from iteration  $\ell$  onwards. Notice that (16) can be evaluated only after seeing the incoming bit pattern at iteration  $\ell$  to obtain  $u^{(\ell)}$  and  $v^{(\ell)}$ . This makes unique decoding impossible, since, assuming that unique decoding was successfully performed up to iteration  $\ell - 1$  at the receiver such that  $u^{(i)}$  and  $v^{(i)}$  are known for all  $i = 1, \dots, \ell - 1$ , decoding cannot identify which codebook was used at iteration  $\ell$  due to the lack of knowledge of  $u^{(\ell)}$  and  $v^{(\ell)}$ . This suggests that, for unique decoding, the codebook at iteration  $\ell$  must be identified without relying on  $u^{(\ell)}$  and  $v^{(\ell)}$ , which can be realized by using a bounding technique. Namely, in a *pessimistic* assumption that the shortest input bits are mapped to the longest output symbols defined in  $\mathcal{C}_1$  at iteration  $\ell$ , we can find the lower bound of the available symbols and the upper bound of the required symbols as

$$\underline{\gamma}_{\text{Ava}}^{(\ell)} := T - t^{(\ell-1)} - v_{\max}, \quad (17)$$

and

$$\overline{\gamma}_{\text{Req}}^{(\ell)} := \left\lceil \frac{S - s^{(\ell-1)} - u_{\min}}{R_2} \right\rceil, \quad (18)$$

where  $u_{\min} := \min_n u_n$  and  $v_{\max} := \max_n v_n$ . Now, without knowledge of  $u^{(\ell)}$  and  $v^{(\ell)}$ , the overflow-preventing condition (16) can be conservatively examined by

$$\underline{\gamma}_{\text{Ava}}^{(\ell)} \geq \overline{\gamma}_{\text{Req}}^{(\ell)}, \quad (19)$$

since  $\gamma_{\text{Ava}}^{(\ell)} \geq \underline{\gamma}_{\text{Ava}}^{(\ell)}$  and  $\overline{\gamma}_{\text{Req}}^{(\ell)} \geq \gamma_{\text{Req}}^{(\ell)}$ .

**Theorem 4.** *In successive PCDM encoding process, frame overflow can be avoided by switching the code from  $\mathcal{C}_1$  to  $\mathcal{C}_2$  at the earliest iteration  $\ell$  that does not fulfill (19).*

*Proof:* If (19) is fulfilled at  $\ell = 1$ , we can use  $\mathcal{C}_1$  at  $\ell = 1$  without overflow. Otherwise, we can avoid overflow by using  $\mathcal{C}_2$  for encoding at every  $\ell = 1, \dots$ , since  $\lceil S/R_2 \rceil \leq T$  by (15). Assume that  $\mathcal{C}_1$  was used at  $\ell = i - 1$ , fulfilling (19), hence ensured that overflow will not occur if we switch to  $\mathcal{C}_2$  at iteration  $i$ . If (19) is fulfilled also at  $\ell = i$ , we keep using  $\mathcal{C}_1$  at  $\ell = i$ , since encoding with  $\mathcal{C}_2$  at every  $\ell \geq i + 1$  suffices to avoid overflow, otherwise, we switch to  $\mathcal{C}_2$  at  $\ell =$

---

**Algorithm 2** Framing of a prefix-free code

---

**Input:**  $\mathcal{C}_1, \mathcal{C}_2$ , a source bit frame  $\mathbf{b} \in \mathcal{B}^S$

**Output:** A code letter frame  $\mathbf{x} \in \mathcal{X}_{M\text{-ASK}}^T$

*Initialization:*

$\ell \leftarrow 0, s^{(\ell)} \leftarrow 0, t^{(\ell)} \leftarrow 0.$

```

1: repeat
2:    $\ell \leftarrow \ell + 1$ 
3:   if  $\underline{\gamma}_{\text{Ava}}^{(\ell)} \geq \overline{\gamma}_{\text{Req}}^{(\ell)}$  then
4:     Encode the current  $u^{(\ell)}$ -bit segment of  $\mathbf{b}$  using  $\mathcal{C}_1$ 
       and produce a  $v^{(\ell)}$ -symbol segment of  $\mathbf{x}$ .
5:      $s^{(\ell)} \leftarrow s^{(\ell-1)} + u^{(\ell)}.$ 
6:      $t^{(\ell)} \leftarrow t^{(\ell-1)} + v^{(\ell)}.$ 
7:   else
8:     Encode the current and all the subsequent bits of  $\mathbf{b}$ 
       using  $\mathcal{C}_2$  to fill  $\mathbf{x}$ .
9:      $s^{(\ell)} \leftarrow S.$ 
10:     $t^{(\ell)} \leftarrow t^{(\ell-1)} + \lceil \frac{S - s^{(\ell-1)}}{R_2} \rceil.$ 
11:   end if
12: until  $s^{(\ell)} < S$ 
13: if  $t^{(\ell)} < T$  then
14:   Fill the last  $T - t^{(\ell-1)}$  symbols of  $\mathbf{x}$  with 1.
15: end if
16: return  $\mathbf{x}$ 

```

---

$i$  without overflow by assumption. This completes proof by mathematical induction. ■

**Theorem 5.** *PCDM symbols framed by using Theorem 4 can be uniquely decoded.*

*Proof:* At  $\ell = 1$ , it is trivial to see that a decoder can identify a proper decoding code using (19), which allows for unique decoding and gives knowledge of  $u^{(1)}$  and  $v^{(1)}$ . Assume that  $u^{(\ell)}$  and  $v^{(\ell)}$  for all  $\ell = 1, \dots, i - 1$  are known at the beginning of decoding iteration  $\ell = i$ . Then, by assessing (19) at  $\ell = i$ , we identify the decoding code at iteration  $\ell = i$ . This enables unique decoding at  $\ell = i$  and provides  $u^{(i)}$  and  $v^{(i)}$ . This completes proof by mathematical induction. ■

In case where *underflow* occurs, i.e., if encoding of  $S$  bits is finished using less than  $T$  symbols, the encoder can simply fill the unoccupied slots in the output frame with dummy symbols of the smallest energy, e.g.,  $\mathcal{X}_1 = 1$  for the  $M$ -ASK alphabet. The decoder can discard these dummy symbols after  $T$  bits are all decoded. There may also be incidents at the end of encoding that need minor manipulations as follows. At the last encoding iteration, it is possible that there is no sourceword in the dictionary that matches perfectly with the input bits. In this case, there must be multiple sourcewords whose  $u'$ -bit prefix matches perfectly with the input bits, where  $u'$  denotes the length of the last remaining input bits, hence an encoder can set a rule for unique encoding; e.g., it can pick the uppermost codeword in such a case. Unique decoding is straight-forward. The framing algorithm is summarized in Algorithm 2.



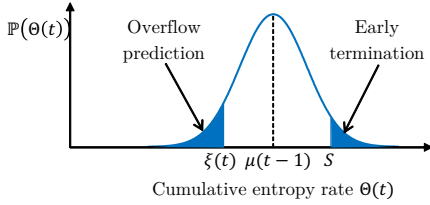


Fig. 10. Approximated Gaussian distribution of the cumulative entropy rate at the  $t$ -th symbol.

### B. Analysis of Fixed-Length Penalty by Gaussian Approximation

Suppose that a prefix-free encoder produces an entropy rate  $r_n$  using the  $n$ -th codeword  $\mathbf{x}_n$  of a size- $N$  code  $\mathcal{C}_1$ , given by  $r_n := \frac{u_n}{N}$ . The probability of occurrence of  $r_n$  equals  $q_n := \frac{p_n v_n}{\sum_{i=1}^N p_i v_i}$ , i.e., the probability that the encoder's output symbol at a certain time belongs to codeword  $\mathbf{x}_n$ . Without a fixed-length constraint, the expected entropy rate of code  $\mathcal{C}_1$ , previously expressed as (2), can alternatively be calculated as  $R_1 = \mathbb{E}_{\mathbf{q}}(R)$ , where  $R$  is a random variable taking values on the ordered set  $\{r_1, \dots, r_N\}$ , with a PMF  $\mathbf{q} := [q_1, \dots, q_N]^T$ . For example, with the V2V code in Tab. I (c), an entropy rate in  $\mathbf{r} := [r_1, \dots, r_N]^T \approx [0.14, 0.43, 0.5, 0.6, 1, 1.67, 3, 6]^T$  is observed at the encoder's output with a PMF  $\mathbf{q} \approx [0.57, 0.143, 0.122, 0.102, 0.041, 0.015, 0.005, 0.003]^T$ , which yields  $R_1 \approx 0.361$  on average. Suppose now that a fixed-length constraint is imposed by framing. We consider the *ensemble* of symbol frames and assume that all symbols encoded by  $\mathcal{C}_1$  are independent and identically distributed (IID). Also, though the true entropy rate of a symbol is a discrete random variable, we approximate the entropy rate by a continuous Gaussian random variable with mean  $R_1$  and variance  $S^2 := \mathbb{E}_{\mathbf{q}}(R^2) - R_1^2$ ; i.e.,  $R \sim \mathcal{N}(R_1, S^2)$ . In this case, the entropy rate accumulated up to the  $t$ -th symbol also follows a Gaussian distribution  $\mathcal{N}(tR_1, t\sigma^2)$ , if there has been neither overflow prediction nor early termination of encoding by  $\mathcal{C}_1$  until the  $(t-1)$ -th symbol. To take into account overflow and early termination, we notice that (17) and (18) at the  $t$ -th output symbol can respectively be transformed into  $\gamma_{\text{Ava}}(t) := T - (t-1) - v_{\text{max}}$  and  $\gamma_{\text{Req}}(t) := \left\lceil \frac{S - \Theta(t-1) - u_{\text{min}}}{R_2} \right\rceil$ , where  $\Theta(t)$  is a random variable representing the *cumulative entropy rate* at the  $t$ -th output symbol.

However, characterization of exact  $\Theta(t)$  becomes infeasible as the overflow and early termination probabilities increase with  $t$ , hence we approximate  $\Theta(t)$  for all  $t = 1, \dots, T$  again by a Gaussian random variable with mean  $\mu(t)$  and variance  $\sigma^2(t)$  such that  $\Theta(t) \sim \mathcal{N}(\mu(t), \sigma^2(t))$  whose evolution over  $t$  is mathematically tractable, as shown in Fig. 10. Then, on condition that code  $\mathcal{C}_1$  is still being used at the  $t$ -th symbol, i.e., on condition that no overflow prediction and early termination has been made before the  $t$ -th symbol, the probability of an overflow prediction at the  $t$ -th symbol is

$$\begin{aligned} \mathbb{P}(\gamma_{\text{Req}}(t) > \gamma_{\text{Ava}}(t)) &\approx \mathbb{P}(S - \Theta(t-1) - u_{\text{min}} - R_2(T - t) > 0) \\ &= \mathbb{P}(\Theta(t-1) < \xi(t)), \quad (20) \\ &= F(\xi(t) | \mu(t-1), \sigma^2(t-1)) \quad (21) \end{aligned}$$

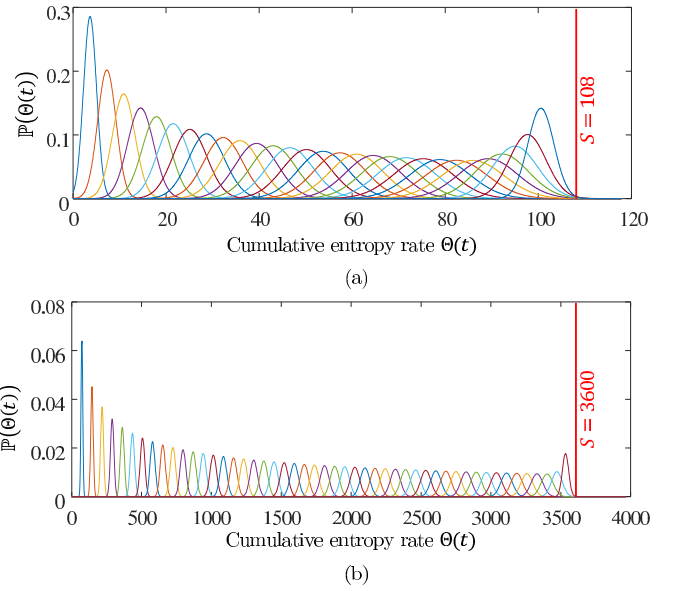


Fig. 11. Evolution of the distribution of the cumulative entropy rate: (a)  $S = 108, T = 300, t = 10k$ , and (b)  $S = 3600, T = 10000, t = 200k$ , for positive integers  $k$ .

where, in (20), an overflow threshold is defined by  $\xi(t) := R_2(t - T - 1 + v_{\text{max}}) + S - u_{\text{min}}$ , and  $F(\cdot | \mu, \sigma^2)$  in (21) denotes Gaussian cumulative distribution function (CDF) with mean  $\mu$  and variance  $\sigma^2$ . Equation (20) gives insight into the behavior of the proposed framing method, since it indicates that overflow is predicted if the entropy rate accumulated until the  $(t-1)$ -th symbol is less than a threshold  $\xi(t)$  that increases linearly with  $t$ . Here,  $\mu(t)$  and  $\xi(t)$  are both linear in  $t$  with slopes  $R_1$  and  $R_2$ , respectively, and since  $R_1 < R_2$  by the framing rule, the probability of overflow prediction in (20) gradually increases with  $t$ . Recall, however, that this is a *conditional* probability, given no overflow prediction and early termination prior to symbol  $t$ .

In order to take into account the history of previous overflow predictions and early terminations, let  $\Phi_{\text{Swi}}(t)$  and  $\Phi_{\text{End}}(t)$  denote the cumulative overflow prediction probability and cumulative early termination probability at symbol  $t$ . Then, the *unconditional* probability that overflow is predicted at symbol  $t$  is

$$\begin{aligned} \phi_{\text{Swi}}(t) &:= (1 - \Phi_{\text{Swi}}(t-1) - \Phi_{\text{End}}(t-1)) \\ &\quad \times F(\xi(t) | \mu(t-1), \sigma^2(t-1)). \quad (22) \end{aligned}$$

And the probability of early termination at symbol  $t$  is

$$\begin{aligned} \phi_{\text{End}}(t) &:= (1 - \Phi_{\text{Swi}}(t-1) - \Phi_{\text{End}}(t-1)) \\ &\quad \times (1 - F(S | \mu(t-1), \sigma^2(t-1))). \quad (23) \end{aligned}$$

It is straightforward to see that their cumulative probabilities are obtained by  $\Phi_{\text{Swi}}(t) = \sum_{i=1}^t \phi_{\text{Swi}}(i)$  and  $\Phi_{\text{End}}(t) = \sum_{i=1}^t \phi_{\text{End}}(i)$ . From the initial conditions  $\Phi_{\text{Swi}}(0) = 0$  and  $\Phi_{\text{End}}(0) = 0$ , the cumulative probabilities can be evaluated in an iterative manner from symbol 1. When evaluating (22) and (23), we have the initial conditions  $\mu(0) = 0$  and  $\sigma^2(0) = 0$ , and  $\mu(t)$  and  $\sigma^2(t)$  for  $t > 0$  can be obtained using the update rule (see Fig. 10)  $\mu(t) =$

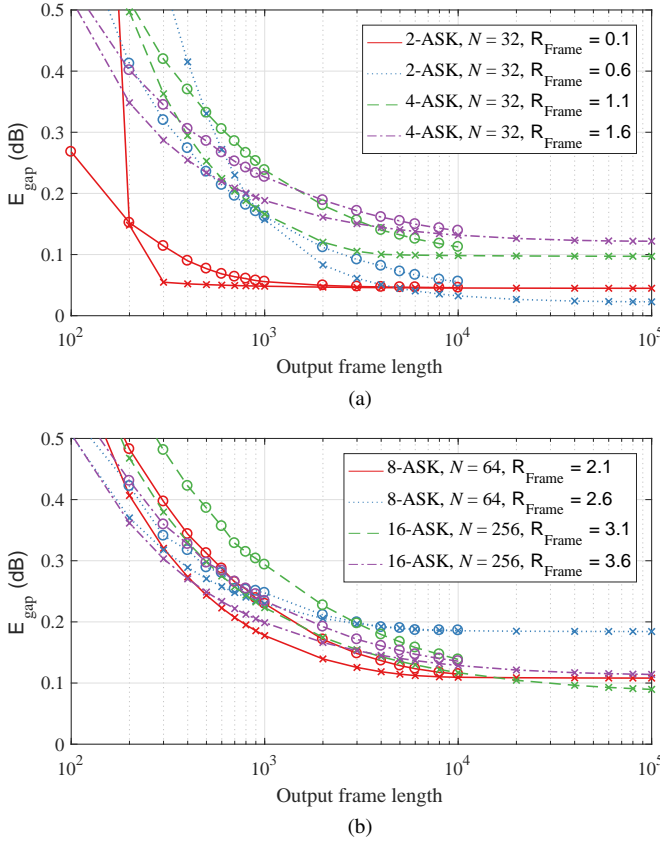


Fig. 12. Energy gap due to framing of (a) V2V codes for the 2- and 4-ASK alphabets, and (b) V2F codes for the 8- and 16-ASK alphabets. Cross and circle markers show the results of GA analysis and MC simulations, respectively.

$\int_{\xi(t-1)}^S \theta \frac{f(\theta | \mu(t-1), \sigma^2(t-1))}{\alpha} d\theta + R_1$ , and  $\sigma^2(t) = \int_{\xi(t-1)}^S (\theta - \mu(t))^2 \frac{f(\theta | \mu(t-1), \sigma^2(t-1))}{\alpha} d\theta + S^2$ , where  $f(\cdot | \mu, \sigma^2)$  denotes Gaussian probability density function (PDF) with mean  $\mu$  and variance  $\sigma^2$ , and  $\alpha$  is a normalization factor defined by  $\alpha := \int_{\xi(t-1)}^S f(\theta | \mu(t-1), \sigma^2(t-1)) d\theta$ .  $\mu(t)$  and  $\sigma^2(t)$  can be efficiently evaluated by numerical integration methods [29].

Figure 11 shows the evolution of a cumulative entropy rate  $\Theta(t)$ , when we use the aforementioned Gaussian approximation (GA) for the V2V code in Tab. I (c). It realizes a fixed entropy rate  $R_{\text{Frame}} = 0.36$  from a probabilistic entropy rate  $R$  with mean  $R_1 \approx 0.361$  and variance  $S^2 = 0.195$ . Each small Gaussian PDF represents a PDF of the cumulative entropy rate measured at the output symbol  $t$ , where  $t$  increments from 10 in a step size of 10 in (a), and from 200 in a step size of 200 in (b). The variance of the Gaussian PDF grows with  $t$  at first, which is expected with little effect from the fixed-length constraint, then begins to decrease near the end of the frame as the probabilities of overflow prediction and early termination emerge. By comparing Figs. 11 (a) and (b), it can be seen that a large frame length reduces the impact of framing on the loss of energy efficiency, as will be quantitatively shown below.

The average energy per symbol under framing can be

estimated by GA as

$$E_{\text{Frame}} = \frac{1}{T} \sum_{t=1}^T \left[ (1 - \Phi_{\text{Swi}}(t) - \Phi_{\text{End}}(t-1)) E_1 + \Phi_{\text{Swi}}(t) E_2 + \Phi_{\text{End}}(t-1) \right], \quad (24)$$

where  $E_1$  and  $E_2$  denote the average energy per symbol generated by  $C_1$  and  $C_2$ , respectively. The energy gap of the prefix-free codes is depicted in Fig. 12, where the codes are selected to support various fixed entropy rates  $R_{\text{Frame}}$  ranging from 0.1 to 3.6 in a granularity of 0.5. The energy gap is estimated by GA, and also by Monte Carlo (MC) simulations, averaged over 10000 frames created from random equiprobable source bits. GA provides very close results to MC simulations as the output frame length increases, in a significantly short time. There exists a trade-off between the frame length and the energy efficiency, and a good compromise seems to be made between a few hundreds and a few thousands of the output frame length. In the limit of the frame length, prefix-free codes approach the ideal energy efficiency of the MB PMFs to within 0.2 dB, even with framing.

## V. RATE-ADAPTABLE PCDM IN AWGN CHANNEL

We evaluate performance of rate-adaptable PCS in the AWGN channel, realized by PCDM with the PAS architecture, as shown in Fig. 13. Fixed-length PCDM is implemented using size-32 V2V prefix-free codes with an output frame length of 10000. The codes are chosen to achieve the entropy rates  $R_{\text{Frame}} \in \{0.1, 0.2, \dots, 0.9\}$  with the 2-ASK alphabet and  $R_{\text{Frame}} \in \{1.2, 1.3, \dots, 1.9\}$  with the 4-ASK alphabet. The maximum IR in bits per probabilistically shaped (PS)- $M$ -QAM symbol can be calculated as  $R_{\text{PS-}M\text{-QAM}} = 2 \left[ R_{\text{Frame}} + \left( 1 - (1 - R_c) \frac{\log_2 M}{2} \right) \right]$ , where  $R_c$  denotes the channel code rate (see (30) in [12]). We use a tail-biting spatially-coupled low-density parity-check (SC-LDPC) code of length 28032 and rate  $R_c = 5/6$ , constructed based on [30], which has a quasi-cyclic structure consisting of size-64 circulant sub-matrices. Normalized min-sum decoding is performed with an iteration limit of 30. The IRs of  $R_{\text{PS-16-QAM}} \in \{1.53, 1.73, \dots, 3.13\}$  and  $R_{\text{PS-64-QAM}} \in \{3.4, 3.6, \dots, 4.8\}$  are obtained with the selected V2V codes and  $R_c = 5/6$ , as shown in parentheses at the top of Fig. 13. The cost of rate adaptation is a size-32 codebook per IR. The bit error rate (BER) and frame error rate (FER) performance is measured as a function of  $E_s/N_0$ , with  $E_s$  being energy per symbol and  $N_0$  being noise variance per two dimensions. For comparison, also shown is the performance of uniform 8-QAM, whose constellation is  $C_3$  of [31] with generalized mutual information-maximizing bit labels, and with uniform square 16-QAM. At a channel frame error rate (FER) of  $10^{-3}$ , PCDM achieves approximately 1.1 dB and 0.65 dB of *shaping gain* at IRs of  $\sim 2.5$  bits/symbol and  $\sim 3.4$  bits/symbol, respectively.

## VI. CONCLUSION

We created a wide range of entropy rates with a very fine granularity using tiny prefix-free codes. In particular, we constructed optimal V2F codes of size  $\leq 4096$  with the 2-, 4-, 8-,

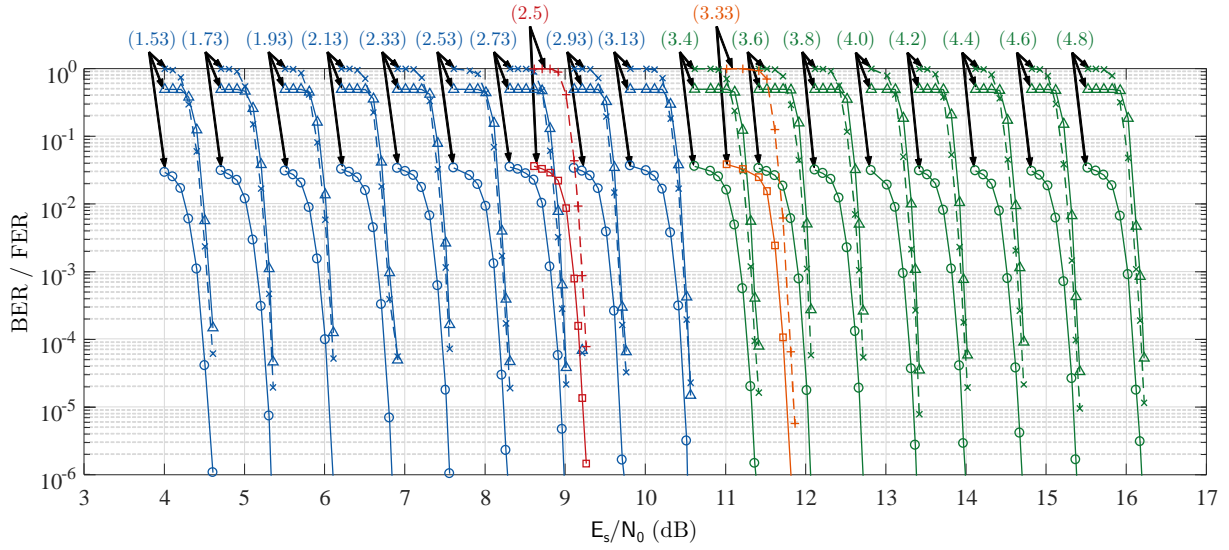


Fig. 13. Bit error rate (BER) and (channel code's) frame error rate (FER) of uniform QAM and PS-QAM realized by PCDM. Square and plus markers indicate the BER and FER of uniform QAM, respectively. Circle and triangle markers show the BER of PS-QAM before and after prefix-free decoding, respectively, and cross markers the FER of PS-QAM before prefix-free decoding.

and 16-ASK alphabets, optimal in the sense that no other code of the same size can achieve a lower energy per code letter for the same entropy rate. We also enumerated all of the optimal F2V codes and many near-optimal V2V codes of size  $\leq 32$  with the 2- and 4-ASK alphabets. Selected codes approach the theoretic maximum energy efficiency to within 0.13 dB across the entropy rate from 0.1 bits/symbol to 3.9 bits/symbol in a step size less than 0.16 bits/symbol. Diversity of the entropy rates and near-optimal energy efficiency show that PCDM is suitable for rate-adaptable PCS. Its implementation cost is a small look-up table for each entropy rate. We also proposed a framing method to implement fixed-rate transmission with variable-rate prefix-free coding, and proved that the suggested framing enables unique prefix-free decoding. We gave insights into the evolution of successive prefix-free encoding process under framing by using GA to analyze the fixed-length penalty. Using GA analysis and MC simulations, we showed that the penalty caused by framing is negligible when the frame length is large enough. Channel coding simulations in the AWGN channel demonstrate that the PCDM-based PS-QAM under framing achieves an SNR gain up to 1.1 dB compared to uniform QAM.

## REFERENCES

- [1] B. P. Tunstall, "Synthesis of noiseless compression codes," Ph.D. dissertation, Georgia Institute of Technology, Linköping, Sweden, 1967.
- [2] B. Varn, "Optimal variable length codes (arbitrary symbol cost and equal code word probability)," *Information and Control*, vol. 19, pp. 289–301, 1971.
- [3] T. C. Hu and A. C. Tucker, "Optimal computer search trees and variable-length alphabetical codes," *SIAM J. Applied Mathematics*, vol. 21, pp. 514–532, 1971.
- [4] G. D. Forney Jr., R. G. Gallager, G. R. Lang, F. M. Longstaff, and S. U. Qureshi, "Efficient modulation for band-limited channels," *IEEE J. Sel. Areas Commun.*, vol. SAC-2, no. 5, pp. 632–647, 1984.
- [5] A. R. Calderbank and L. H. Ozarow, "Nonequiprobable signaling on the Gaussian channel," *IEEE Trans. Inf. Theory*, vol. 36, no. 4, pp. 726–740, 1990.
- [6] G. D. Forney Jr., "Trellis shaping," *IEEE Trans. Inf. Theory*, vol. 38, no. 2, pp. 281–300, 1992.
- [7] J. N. Livingston, "Shaping using variable-size regions," *IEEE J. Sel. Areas Commun.*, vol. 38, no. 4, pp. 1347–1353, 1992.
- [8] F. R. Kschischang and S. Pasupathy, "Optimal nonuniform signaling for Gaussian channels," *IEEE Trans. Inf. Theory*, vol. 39, no. 3, pp. 913–929, 1993.
- [9] D. Raphaeli and A. Gurevitz, "Constellation shaping for pragmatic turbo-coded modulation with high spectral efficiency," *IEEE Trans. Commun.*, vol. 52, no. 3, pp. 341–345, 2004.
- [10] S. Kaimalettu, A. Thangaraj, M. Bloch, and S. W. McLaughlin, "Constellation shaping using LDPC codes," in *Proc. IEEE International Symposium on Information Theory*, 2007, pp. 2366–2370.
- [11] M. C. Valenti and X. Xiang, "Constellation shaping for bit-interleaved LDPC coded APSK," *IEEE Trans. Commun.*, vol. 60, no. 10, pp. 2960–2970, 2012.
- [12] G. Böcherer, F. Steiner, and P. Schulte, "Bandwidth efficient and rate-matched low-density parity-check coded modulation," *IEEE Trans. Commun.*, vol. 63, no. 12, pp. 4651–4665, 2015.
- [13] J. Abrahams, "Variable-length unequal cost parsing and coding for shaping," *IEEE Trans. Inf. Theory*, vol. 44, no. 4, pp. 1648–1650, 1998.
- [14] A. Lempel, S. Even, and M. Cohn, "An algorithm for optimal prefix parsing of a noiseless and memoryless channel," *IEEE Trans. Inf. Theory*, vol. IT-19, pp. 208–214, 1973.
- [15] R. A. Amjad and G. Böcherer, "Fixed-to-variable length distribution matching," in *Proc. IEEE International Symposium on Information Theory*, 2013, pp. 1511–1515.
- [16] V. S.-N. Choi and M. Golin, *Lopsided trees: Analyses, algorithms, and applications*. Berlin, Heidelberg: Springer Berlin Heidelberg, 1996, pp. 538–549.
- [17] M. J. Golin and N. Young, "Prefix codes: Equiprobable words, unequal letter costs," *SIAM J. Comput.*, vol. 25, pp. 1281–1292, 1996.
- [18] M. J. Golin and G. Rote, "A dynamic programming algorithm for constructing optimal prefix-free codes with unequal letter costs," *IEEE Trans. Inf. Theory*, vol. 44, no. 5, pp. 1770–1781, 1998.
- [19] M. J. Golin and J. Li, "More efficient algorithms and analyses for unequal letter cost prefix-free coding," *IEEE Trans. Inf. Theory*, vol. 54, no. 8, pp. 3412–3424, 2008.
- [20] G. Bocherer and R. Mathar, "Matching dyadic distributions to channels," in *Proc. Data Compression Conference*, 2011, pp. 23–32.
- [21] T. H. Cormen, C. Stein, R. L. Rivest, and C. E. Leiserson, *Introduction to Algorithms*, 2nd ed. McGraw-Hill Higher Education, 2001.
- [22] R. P. Stanley, *Catalan Numbers*. Cambridge University Press, 2015.
- [23] N. Dershowitz and S. Zaks, "Enumerations of ordered trees," *Discrete Math.*, vol. 31, no. 1, pp. 9–28, Jan. 1980.
- [24] CVX Research, Inc., "CVX: Matlab software for disciplined convex programming, version 2.1," <http://cvxr.com/cvx>, Mar. 2017.
- [25] M. Grant and S. Boyd, "Graph implementations for nonsmooth convex programs," in *Recent Advances in Learning and*

- Control*. Springer-Verlag Limited, 2008, pp. 95–110, [http://stanford.edu/~boyd/graph\\_dcp.html](http://stanford.edu/~boyd/graph_dcp.html).
- [26] S. Boyd and L. Vandenberghe, *Convex Optimization*. Cambridge University Press, 2004.
  - [27] G. Böcherer, “Capacity-achieving probabilistic shaping for noisy and noiseless channels,” Ph.D. dissertation, RWTH Aachen University, Aachen, Germany, 2012.
  - [28] R. A. Amjad, “Algorithms for simulation of discrete memoryless sources,” Master’s thesis, Technische Universität München, Munich, Germany, 2013.
  - [29] P. J. Davis and P. Rabinowitz, *Methods of numerical integration*. Courier Corporation, 2007.
  - [30] J. Cho and L. Schmalen, “Construction of protographs for large-girth structured LDPC convolutional codes,” in *Proc. IEEE International Conference on Communications*, 2015, pp. 4412–4417.
  - [31] L. Schmalen, A. Alvarado, and R. Rios-Müller, “Performance prediction of nonbinary forward error correction in optical transmission experiments,” *Journal of Lightwave Technology*, vol. 35, no. 4, pp. 1015–1027, 2017.